

New Form Discovery for the Analgesics Flurbiprofen and Sulindac Facilitated by Polymer-Induced Heteronucleation

ADAM L. GRZESIAK, ADAM J. MATZGER

Department of Chemistry and the Macromolecular Science and Engineering Program, The University of Michigan, Ann Arbor, Michigan 48109-1055

Received 8 November 2006; revised 10 January 2007; accepted 5 February 2007

Published online in Wiley InterScience (www.interscience.wiley.com). DOI 10.1002/jps.20954

ABSTRACT: The selection and discovery of new crystalline forms is a longstanding issue in solid-state chemistry of critical importance because of the effect molecular packing arrangement exerts on materials properties. Polymer-induced heteronucleation has recently been developed as a powerful approach to discover and control the production of crystal modifications based on the insoluble polymer heteronucleant added to the crystallization solution. The selective nucleation and discovery of new crystal forms of the well-studied pharmaceuticals flurbiprofen (FBP) and sulindac (SUL) has been achieved utilizing this approach. For the first time, FBP form III was produced in bulk quantities and its crystal structure was also determined. Furthermore, a novel 3:2 FBP:H₂O phase was discovered that nucleates selectively from only a few polymers. Crystallization of SUL in the presence of insoluble polymers facilitated the growth of form I single crystals suitable for structure determination. Additionally, a new SUL polymorph (form IV) was discovered by this method. The crystal forms of FBP and SUL are characterized by Raman and FTIR spectroscopies, X-ray diffraction, and differential scanning calorimetry. © 2007 Wiley-Liss, Inc. and the American Pharmacists Association *J Pharm Sci* 96:2978–2986, 2007

Keywords: polymorphism; X-ray diffractometry; crystallization; crystal structure; solid-state stability

INTRODUCTION

Research activity seeking methodology for controlling the production of a given solid phase has drastically increased in recent years, in large part due to intellectual property rights and quality control regulations in the pharmaceutical industry.^{1–3} Crystal polymorphism can have a profound effect on solid-state properties and, because of potential differences in bioavailability, is of key importance in the manufacture of drugs. Traditional methods of controlling the phenomenon of polymorphism,^{4–6} including modification of crys-

tallization conditions, such as changing solvent, temperature of crystallization, extent of supersaturation, or melt crystallization, are often not efficient at discovering new polymorphs or controlling phase production. However, several recent methods have proven effective in selective production of known forms.^{7–17} Moreover, the polymer-induced heteronucleation approach has been successful in the discovery of novel pharmaceutical polymorphs and has also facilitated the growth of single crystals of small molecules,^{16,17} extended networks,¹⁸ and inorganic complexes¹⁹ directly in the presence of insoluble polymers. This is highly desirable for structure determination of both stable and metastable polymorphs because it sheds light on the intermolecular interactions stabilizing the crystal structure and gives unambiguous proof of the existence of a new

Correspondence to: Adam J. Matzger (Telephone: 734-615-6627; Fax: 734-615-8553; E-mail: matzger@umich.edu)

Journal of Pharmaceutical Sciences, Vol. 96, 2978–2986 (2007)
© 2007 Wiley-Liss, Inc. and the American Pharmacists Association

crystal form. A self-consistent set of spectroscopic, calorimetric, and powder X-ray diffraction (PXRD) data can then be correlated with the corresponding structure allowing more accurate phase identification during manufacture.

The polymorphism of flurbiprofen (FBP) and sulindac (SUL) has been studied for decades yielding three polymorphs of each drug.^{20–24} In the case of FBP, two polymorphs are stable at ambient conditions, while the other is reported to be stable only when crystallized between a cover slip and glass slide or in an aluminum pan.²² Furthermore, only the crystal structure of FBP form I has been determined.²⁵ Similarly, of the three SUL polymorphs, all of which are reported to be stable at ambient conditions,^{23,24} the crystal structure of only form II has been elucidated.²⁶ In this case, the structure determined is actually of the thermally less stable form II and the data are not of sufficient quality for accurately characterizing key intermolecular interactions. Here the crystallization of the two polymorphic pharmaceuticals FBP and SUL is examined utilizing the polymer-induced heteronucleation approach to demonstrate its utility in producing new crystalline forms and single crystals suitable for structural characterization.

EXPERIMENTAL

Materials

Commercial FBP (TCI, Portland, OH) and SUL (Sigma, St. Louis, MO) were used as supplied. Solvents, purchased from Fisher Scientific (Fairlawn, NJ) with the exception of ethanol (Pharmco Products, Inc., Brookfield, CT), were used directly. Commercial polymers were purchased from Scientific Polymer Products, Inc. (Ontario, NY).

Crystallization of FBP and SUL

FBP (300 mg) was dissolved in methanol (15 mL), ethanol (15 mL), ethyl acetate (15 mL) acetonitrile (15 mL), 2-propanol (15 mL), and heptane (200 mg/15 mL with heating) and the entire solution dispensed evenly among the 96 wells of a microtiter plate, each of which contained a few milligram of a single polymer. SUL (100 mg) was dissolved in methanol (10 or 15 mL), ethanol (15 mL), acetone (15 mL), chloroform (15 mL), ethyl acetate (15 mL with heating), acetonitrile (20 mL with heating), and 2-propanol (15 mL with

heating) and the entire solution was dispensed as described above. For solutions that required heating for dissolution, the solution was cooled to room temperature prior to dispensing and no crystallization was observed upon cooling. Crystallization proceeded upon evaporation of the solvent at room temperature under a crystallizing dish. A library of commercial polymers was employed to maximize heteronucleant diversity and results are only reported for those crystallizations in which the polymer did not dissolve to an appreciable extent, in order to favor a heteronucleation mechanism of crystal form production.

X-Ray Diffraction

Single crystal X-ray diffraction data were recorded on a Bruker SMART 1K CCD-based X-ray diffractometer equipped with an LT-2 low temperature device and normal focus Mo-target X-ray tube ($\lambda = 0.71073 \text{ \AA}$) operated at 2000 W power (50 kV, 40 mA). Data were corrected for absorption and the structures were solved and refined using the Bruker SHELXTL software package (version 6.12). All nonhydrogen atoms were refined anisotropically with the hydrogen atoms placed in idealized positions or located on a difference map and allowed to refine. The crystallographic data for SUL form I, FBP hydrate, and FBP form III have been deposited with the Cambridge Crystallographic Data Centre as CCDC Nos. 625435, 625436, and 625437, respectively. These data can be obtained free of charge from the CCDC, 12 Union Road, Cambridge CB2 1EZ, UK (fax: +44-1233-336033, e-mail: data_request@ccdc.cam.ac.uk, or www.ccdc.cam.ac.uk/products/csd/request).

PXRD was performed on a Rigaku R-Axis Spider diffractometer equipped with a $\text{CuK}\alpha$ source ($\lambda = 1.5406 \text{ \AA}$) operated at 2000 W power (50 kV, 40 mA) and an image plate detector. Powder samples were mounted on a standard goniometer head equipped with a Nylon loop and affixed with Apiezon-M grease. Typical scans were 30 min with ω oscillating from 80 to 140° at 1°/sec, φ spinning at a rate of 10°/sec, and χ fixed at 30° to remove the effects of preferred orientation.

Vibrational Spectroscopy

Raman spectra were obtained using a Renishaw inVia Raman Microscope equipped with a Leica microscope, RenCam CCD detector, 785 nm diode

laser, 1200 lines/mm grating, and 50 μm slit. Spectra were collected in either extended scan mode with a range of 100–3200 cm^{-1} or static scan mode centered at 420 cm^{-1} . Calibration was performed using a silicon standard. Fourier transform infrared (FTIR) spectra were collected in transmission mode in KBr pellets utilizing a Perkin-Elmer Spectrum BX FTIR system. The scan range was 400–4000 cm^{-1} , using eight scans per spectrum with a resolution of 2 cm^{-1} . Raman spectroscopy of the KBr pellets confirmed that no polymorphic transformation had occurred during grinding or compression for the polymorphs tested. Raman and FTIR spectra were analyzed using the ACD/SpecManager (v8.11) software package.

Differential Scanning Calorimetry (DSC)

Thermograms of the samples were recorded on a TA Instruments Q10 DSC. The thermal behavior of the samples, placed in sealed aluminum pans, was studied under a nitrogen purge with heating rates of 5°C/min, covering a temperature range from 30 to 130°C for FBP and 40 to 220°C for SUL. The instrument was calibrated with an indium standard.

Thermomicroscopy

Melting behavior was determined using a Mettler Toledo FP82HT hot stage connected to an FP90 control processor and viewed under crossed polarizers with a Leica DMLP microscope. Heating rates were typically 1.0 or 5.0°C/min.

Thermogravimetric Analysis (TGA)

Samples were heated from room temperature to 400°C in a nitrogen atmosphere at a rate of 10°C/min utilizing a TA Instruments Q50 TGA. The instrument was calibrated with nickel and alumel standards.

RESULTS AND DISCUSSION

Flurbiprofen

To explore the utility of the polymer-induced heteronucleation approach for selectively crystallizing polymorphs of the analgesic FBP and facilitating single crystal growth, crystallization

was performed in the presence of polymer heteronuclei. Raman spectroscopy of FBP crystals revealed four distinct vibrational spectra during high-throughput screening experiments. Three of these were attributed to the known forms I–III of FBP based on Raman spectroscopy, PXRD, and melting behavior compared to results from previous literature characterization.^{20,22} The majority of crystallizations in the presence of polymers (>90%) resulted in the formation of form I with a blade morphology. Form I has a characteristic Raman spectrum (Fig. 1) with peaks at 219, 239, 284, 317, 419, 441, 474, 1128, 1295, and 1518 cm^{-1} and FTIR spectrum with peaks at 575, 698, 766, 1129, 1324, and 1701 cm^{-1} , as well as PXRD pattern with identifiable peaks at $2\theta = 7.1, 10.7, 16.4, 20.4, 23.4,$ and 29.7° (Fig. 2, Tab. 1). The melting behavior of form I on the hot stage with a heating rate of 5°C/min revealed a melting point of 115.5°C. DSC was performed to quantify the melting behavior of form I and this revealed an endotherm of melting with an onset temperature of 115.0(2)°C and melting enthalpy of 29.1(4) kJ/mol (Fig. 3, Tab. 2).

Needle-shaped form II crystals were identified from several polymers including chlorosulfonated polyethylene, polysulfone, and poly(vinyl alcohol) from methanol solutions, 1,2-polybutadiene from ethanol solutions, methyl vinyl ether/maleic acid copolymer from 2-propanol solutions, and chlorinated polyethylene from acetonitrile solutions. However, large quantities of form II were more easily obtained by seeding supersaturated hexanes solutions with seed crystals grown directly from polymers. This method was more reliable than the literature method of crystallization of supersaturated heptane solutions, which is

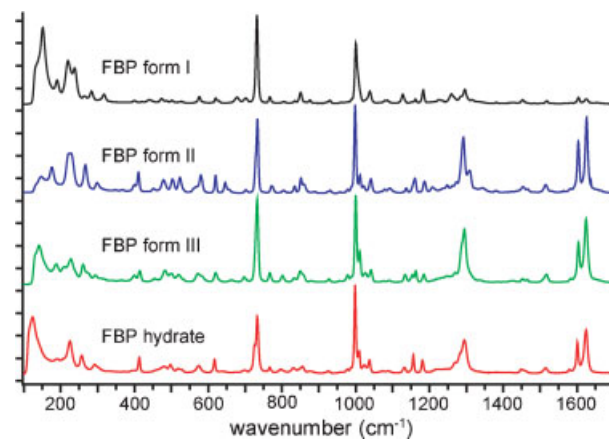


Figure 1. Raman spectra of the crystal forms of flurbiprofen.

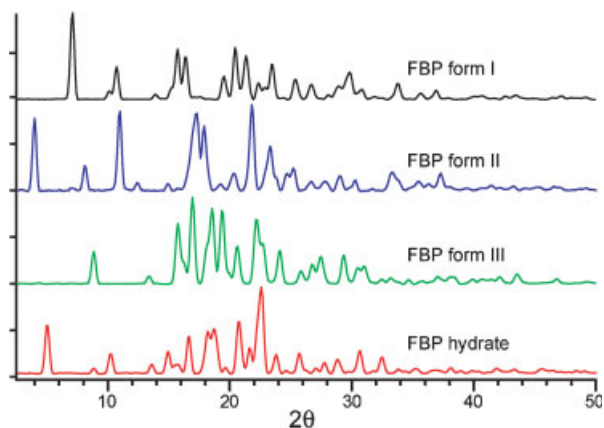


Figure 2. PXRD patterns of the crystal forms of flurbiprofen.

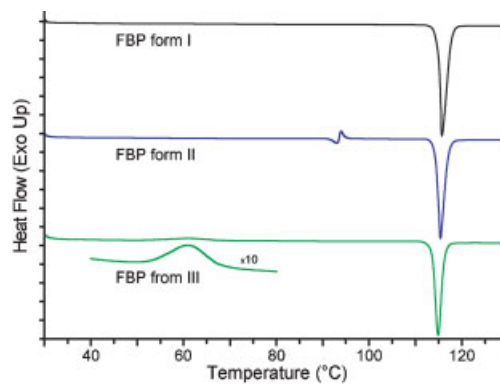


Figure 3. DSC thermograms of forms I, II, and III of flurbiprofen.

Table 1. PXRD Data for the Crystal Forms of Flurbiprofen and Sulindac

FBP form I		FBP form II		FBP form III		FBP hydrate		SUL form I		SUL form II		SUL form IV	
2θ (°)	I/I ₀ (%)	2θ (°)	I/I ₀ (%)	2θ (°)	I/I ₀ (%)	2θ (°)	I/I ₀ (%)	2θ (°)	I/I ₀ (%)	2θ (°)	I/I ₀ (%)	2θ (°)	I/I ₀ (%)
7.1	100	4.0	73.9	8.9	37.4	5.0	71.4	7.1	5.7	9.6	54.8	6.2	11.8
10.1	9.9	8.1	29.5	13.4	8.7	8.9	7.7	10.7	36.4	12.3	16.2	7.6	11.0
10.7	37.6	11.0	92.6	15.8	69.6	10.2	29.4	11.8	10.9	14.0	24.1	12.5	20.0
13.9	5.5	12.4	9.1	17.0	100	13.6	14.0	13.0	35.8	15.1	28.5	13.3	32.7
15.7	57.6	14.9	8.0	18.5	77.4	15.0	32.6	14.3	36.1	16.4	26.8	15.3	65.7
16.4	48.4	17.3	91.5	19.4	84.9	15.7	13.8	17.5	23.8	18.5	100	16.5	42.0
19.5	26.3	17.9	74.4	20.7	43.8	16.7	54.9	18.5	100	19.4	8.3	17.8	32.7
20.4	59.5	19.2	6.8	22.2	75.3	18.2	62.9	19.8	24.6	21.4	81.6	18.7	18.4
21.3	49.8	20.3	19.3	22.7	47.5	18.7	66.5	21.3	63.0	22.5	29.4	19.7	17.6
22.3	18.6	21.8	100	24.2	38.6	19.7	8.7	22.7	18.1	24.0	88.2	21.2	9.8
22.9	13.8	23.3	52.3	25.9	15.1	20.8	77.3	23.9	86.0	24.9	28.1	22.2	100
23.4	40.5	24.7	19.9	26.8	22.6	21.6	37.9	25.6	19.5	26.3	30.7	23.9	5.7
25.3	23.9	25.2	26.7	27.5	31.8	22.4	100	26.4	51.3	27.1	15.4	25.0	5.7
26.7	17.7	26.7	10.2	29.4	33.4	23.8	28.3	28.5	14.6	28.4	17.5	25.6	13.1
28.1	5.3	27.8	10.2	30.6	18.6	24.6	5.5	29.4	5.4	29.2	9.6	27.6	12.7
28.9	15.4	29.0	17.0	31.1	20.5	25.7	30.3	30.0	9.5	30.2	11.4	29.5	13.1
29.7	29.7	30.3	12.5	32.5	5.2	27.1	8.0	32.8	11.2	30.5	9.2	30.2	14.7
30.8	11.8	33.3	23.3	33.2	6.8	27.8	16.4	33.9	6.6	32.1	8.3	31.0	6.1
33.7	18.4	35.5	11.9	34.7	4.7	28.8	21.0	40.0	8.9	33.0	11.0	32.9	5.3
35.6	7.2	36.3	8.5	37.1	8.7	30.7	34.2	40.7	4.9	34.3	4.4	34.1	5.7
36.9	11.0	37.3	20.5	38.2	8.2	32.5	24.7	48.5	4.0	35.0	13.2	35.7	4.1
40.1	4.1	38.0	6.8	39.9	5.9	33.8	6.6			36.1	7.9	38.7	5.3
40.6	4.6	41.4	5.1	40.7	5.9	35.3	7.6			38.5	7.5		
42.5	4.2	43.3	4.0	41.5	5.6	36.9	5.6			39.9	8.3		
43.4	5.5	46.6	4.0	42.2	8.2	38.1	8.7			40.4	11.0		
47.1	4.4			43.6	11.8	41.9	8.1			41.0	7.5		
51.0	6.0			46.9	6.1	43.3	6.6			43.8	7.5		
						45.6	7.4			44.6	4.4		
						46.5	5.2			48.5	6.1		
										49.3	6.1		

Table 2. Melting/Transition Temperature, Enthalpy of Transition, and Enthalpy of Melting for Flurbiprofen and Sulindac Polymorphs

	Onset of melting or transition (°C)	ΔH_{trans} (kJ/mol)	ΔH_{m} (kJ/mol)
FBP form I	115.0 (2)	–	29.1 (4)
FBP form II	91.5 (1)	–0.28 (3)	28.1 (3)
FBP form III	55.3 (10)	–2.9 (1)	22.4 (13)
SUL form I	190.6 (2)	–	27.6 (1)
SUL form II	185.6 (1)	–	31.1 (1)
SUL form IV	130.8 (31)	–	21.4 (18)

reported as inefficient.²⁰ Form II was characterized by its distinct Raman spectrum with peaks at 221, 228, 299, 411, 452, 479, 1137, 1291, and 1515 cm^{-1} and FTIR spectrum with peaks at 575, 701, 769, 1135, 1339, and 1711 cm^{-1} . Its PXRD pattern exhibits characteristic diffraction at $2\theta = 4.0, 11.0, 17.3, 17.9, 21.8,$ and 23.3° and DSC reveals a 0.28(3) kcal/mol, overall exothermic event with an onset temperature of 91.5(1)°C. This transition corresponds to form II melting and the simultaneous crystallization of form I, which then melts at its expected temperature. This process was confirmed by thermomicroscopy where a transformation was observed between 90 and 96°C and subsequent melting at 115.0°C, which is consistent with form I melting. Raman microscopy of a sample heated to 100°C to allow completion of the transition revealed that the crystal had transformed to form I. The enthalpy of melting of form II was determined to be 28.1(3) kJ/mol and application of the heat-of-transition rule²⁷ reveals a monotropic relationship between forms I and II.

Crystallization of form III, originally reported to be stable only between a glass slide and cover slip,²² was common and highly selective utilizing ethylene/vinyl acetate copolymers and oxidized polyethylene from ethyl acetate, methanol, acetonitrile, and 2-propanol solutions.²⁸ Although transformation to other polymorphs may occur upon standing, many isolated crystals are indefinitely stable at ambient conditions allowing full characterization of pure material by Raman and FTIR spectroscopies, PXRD, DSC, and thermomicroscopy. Characteristic Raman shifts at 207, 228, 295, 415, 454, 483, 1134, 1294, and 1517 cm^{-1} and absorbances in the FTIR at 571, 696, 765, 1131, 1331, 1700, and 1714 cm^{-1} were observed. PXRD shows identifiable peaks at $2\theta = 8.9, 15.8, 17.0, 18.5, 19.4,$ and 22.2° . Single plate-like crystals of form III were obtained by evaporation of an ethyl acetate solution in the presence of

oxidized polyethylene. The single crystal structure of form III was solved (Fig. 4b) in the monoclinic space group $P2_1/c$ with $a = 5.7214(9), b = 38.715(6), c = 5.9808(10)$ Å, $\beta = 111.655(2)^\circ$, $V = 1231.3(3)$ Å³, $Z = 4$. Analysis of the structure reveals identical dimerization of enantiomers through the carboxylic acid group and a similar molecular conformation as observed in the crystal structure of form I,²⁵ except that the position of the fluorine atom is disordered over two positions related by a 180° rotation of the fluorine substituted ring. The packing arrangement of form III is such that a 2.43 Å short C–H...F contact is observed between adjacent molecules when the fluorine is in the higher occupancy position.²⁹ A different C–H...F interaction of 2.27 Å also exists for the lower occupancy position of the disordered fluorine. Additionally, two C–H...O interactions exist at 2.59 and 2.66 Å that, when taken together with the other intermolecular interactions, create sheets of dimers.

It was found that bulk quantities of form III could be produced from the melt on polypropylene in about 50% of crystallizations, which allowed for the first full characterization of this polymorph as pure material. DSC reveals an exothermic polymorphic transition of 2.9(1) kJ/mol to form I between 50 and 70°C. This is consistent with thermomicroscopy experiments where the transformation is observed between 55 and 90°C. Raman spectroscopic analysis of the transformed material confirmed the identity of form I along with the appropriate melting point in the DSC and hot-stage experiments. Therefore, based on the heat-of-fusion and heat-of-transition rules,²⁷ forms I and III are monotropically related; forms II and III are also monotropically related based on the heat-of-fusion rule.

The fourth unique Raman spectrum observed was found with crystals grown from methanol in the presence of poly(*n*-butyl methacrylate), polycaprolactone, chlorinated polyethylene, and

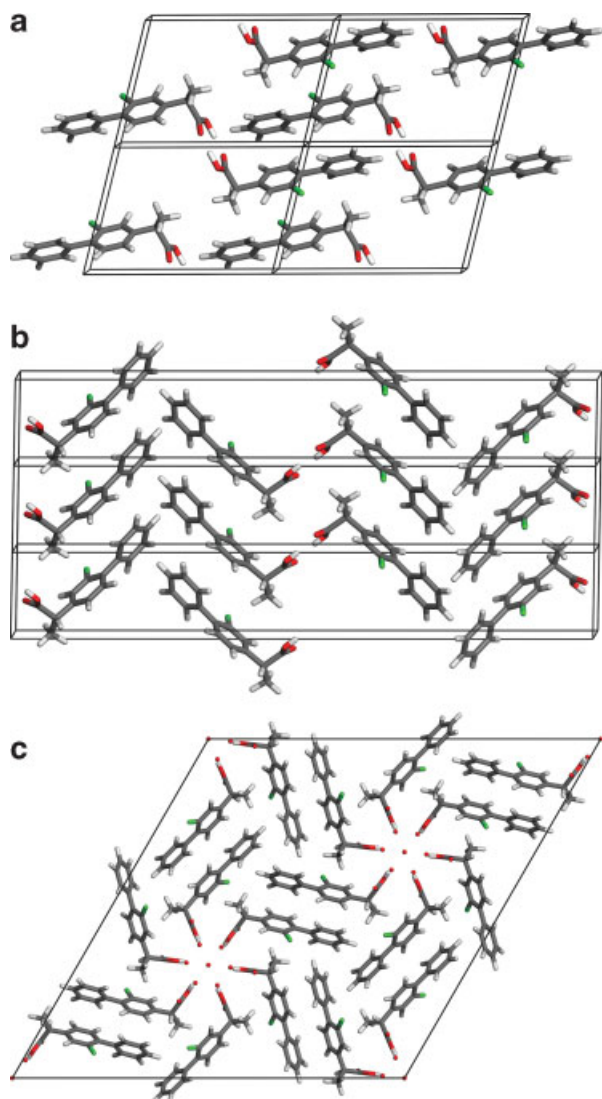


Figure 4. Packing diagrams of (a) form I, (b) form III, and (c) hydrate of flurbiprofen.

styrene butadiene ABA block copolymer as well as the sodium salt of alginic acid and poly(vinyl alcohol) from evaporation of ethanol solutions. The distinguishing peaks in the Raman spectrum were observed at 225, 257, 293, 396, 413, 479, 1131, 1295, and 1515 cm^{-1} . PXRD indicated a new crystalline phase with diffraction lines at $2\theta = 5.0, 16.7, 18.2, 18.7, 20.8, 22.4, \text{ and } 30.7^\circ$. Heating of this form on the hot stage reveals a broad transition between 50 and 90°C, which is found to be a transformation to form I, as verified by Raman microscopy. Moreover, this transition to form I occurs at room temperature when the crystals are allowed to stand for several days and is accelerated upon grinding with KBr and pressing a pellet, which precluded obtaining FTIR

data. Single crystals were grown by slow evaporation (2 days) of an ethanol solution in the presence of the sodium salt of alginic acid and the structure was determined (Fig. 4c). It revealed an unprecedented hydrated FBP form with 3:2 FBP:H₂O stoichiometry that crystallizes in the rhombohedral space group $R\bar{3}$ with the following unit cell parameters: $a = b = 33.589(3), c = 5.8932(7)$ Å, $V = 5757.9(9)$ Å³, $Z = 18$. TGA data show a mass loss of 4.9(1)%, in agreement with the FBP:H₂O ratio observed in the crystal structure. The water molecules, which are disordered in the structure model, reside in channels formed by six FBP molecules. Hydrogen bonding from the carboxylic acid donor to the oxygen of a water is apparent with a distance of 2.29 Å and, although hydrogens on the water molecules are not resolved in the structure, O...O distances of 2.58 Å to the carbonyl and 2.72 Å to the oxygen of the acid indicate the presence of additional hydrogen bonds. The crystallization of this form occurred more frequently with addition of water to FBP solutions in the presence of polymers. However, in the absence of polymers it was not observed upon evaporation of methanol solutions containing added water. Furthermore, when FBP hydrate is stirred in an aqueous solution that is saturated with respect to form I, the hydrate transforms to form I. Therefore, this hydrate is not stable to water.

Sulindac

SUL was crystallized in the same manner as FBP in the presence of a diverse polymer library from a variety of solvents. Many common solvents favor the formation of form II with room temperature evaporation, but 73% of crystallizations from acetone solution in the presence of polymers and several crystallizations from methanol solutions in the presence of Nylons, polyamide resin, styrene/ethylene-butylene ABA block copolymer, and carboxylated vinyl chloride/vinyl acetate copolymer resulted in the nucleation of form I. Large quantities of form I were also obtained by sublimation. This form was identified by its distinctive PXRD pattern (Fig. 5, Tab. 1) with diffraction lines at $2\theta = 7.1, 10.7, 13.0, 18.5, 19.8, \text{ and } 26.4^\circ$, Raman spectrum (Fig. 6) with shifts at 192, 225, 283, 306, 395, 438, 869, 1182, and 1211 cm^{-1} and FTIR peaks at 871, 1008, 1023, 1403, 1602, and 1713 cm^{-1} . The melting behavior of this form^{23,24} consists of a single melt at 191.0°C

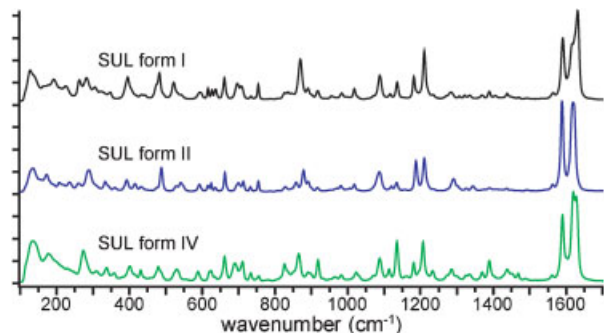


Figure 5. PXRD patterns of forms I, II, and IV of sulindac.

on the hot stage. DSC revealed an onset of melting at 190.6(2)°C with an enthalpy of melting of 27.6(1) kJ/mol (Fig. 7, Tab. 2). Evaporation of methanol solutions in the presence of Nylon 6/9, Nylon 6/10, and styrene/ethylene-butylene ABA block copolymer yielded plate-like single crystals of form I suitable for structure determination by X-ray diffraction. This form was found to crystallize in the monoclinic space group $P2_1/c$ with $a = 12.645(3)$, $b = 7.8887(17)$, $c = 17.788(4)$ Å, $\beta = 104.879(3)^\circ$, $V = 1714.9(6)$ Å³, $Z = 4$. Analysis of the structure of form I reveals hydrogen bonding from the carboxylic acid to the sulfone with a distance of 1.77 Å, which is similar to that found in form II (Fig. 8). Additionally, there is a short C–H...F contact of 2.39 Å and three C–H...O contacts of 2.50, 2.56, and 2.62 Å that, when taken together, create a three-dimensional network of hydrogen bonding.

Blade morphology form II crystals, which are the commercial form of SUL, were the major product crystallized from most solvents utilized, particularly methanol, ethanol, and 2-propanol. Form II has a characteristic Raman spectrum

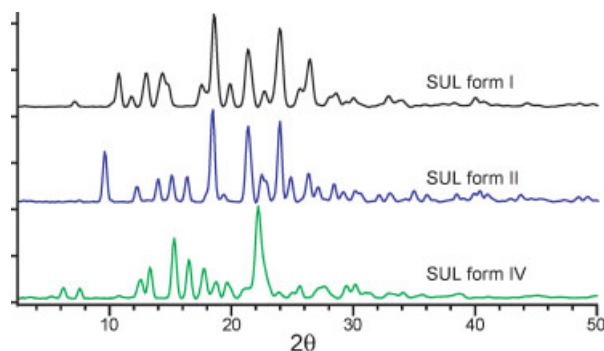


Figure 6. Raman spectra of forms I, II, and IV of sulindac.

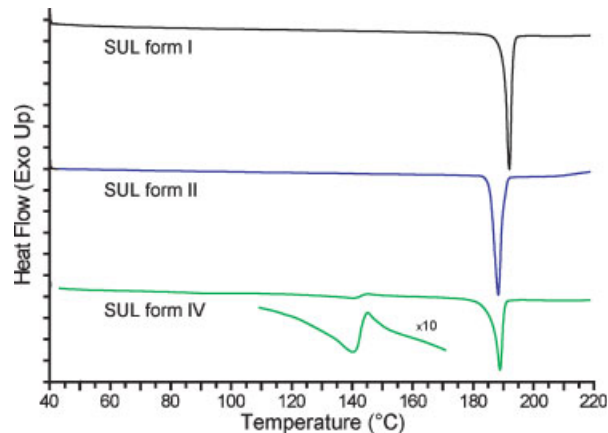


Figure 7. DSC thermograms of forms I, II, and IV of sulindac.

with peaks at 173, 208, 236, 289, 393, 416, 433, 878, 1188, and 1211 cm^{-1} as well as FTIR peaks at 879, 1007, 1019, 1407, 1589, 1603, and 1701 cm^{-1} . It also has distinctive peaks at $2\theta = 9.6, 14.0, 18.5, 21.4, 24.0,$ and 24.9° in the PXRD pattern. The melting point of form II was found to be 187.5°C on the hot stage and DSC showed an onset of melting at 185.6(1)°C and an enthalpy of melting of 31.1(1) kJ/mol, which is in agreement with previously reported data.^{23,24} This indicates an enantiotropic relationship between SUL forms I and II.

Notably absent was form III, which was never produced utilizing the polymer-induced hetero-

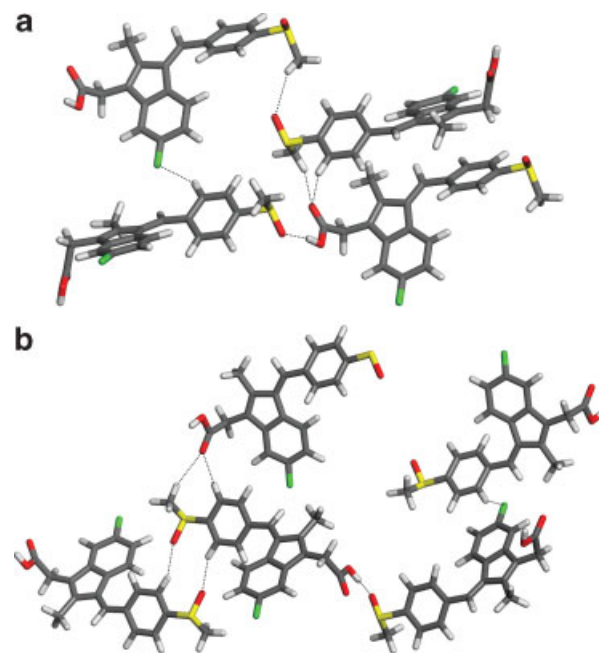


Figure 8. Packing diagrams showing hydrogen bonding in (a) form I and (b) form II of sulindac.

nucleation approach or the literature method.²⁴ However, there was the appearance of needle-shaped crystals with characteristic Raman shifts at 180, 274, 310, 337, 401, 431, 865, 1181, and 1207 cm^{-1} from crystals grown by evaporation of methanol and 2-propanol in the presence of chlorinated polyethylene (42% Cl). The selectivity for this form was greater than 95% in crystallizations from methanol solutions using these conditions, but single crystals were not obtained. FTIR shows distinguishing peaks at 861, 1012, 1027, 1401, 1602, and 1711 cm^{-1} . TGA data showed no mass loss prior to 240°C indicating that there was no solvent in the lattice. Data from PXRD with identifiable peaks at $2\theta = 6.2, 7.6, 13.3, 15.3, 16.5,$ and 22.2° do not match any known patterns proving that this is indeed a new polymorph of SUL (form IV). Upon heating form IV at 5°C/min on the hot stage, it melts and partially recrystallizes to a new form between 140 and 160°C. The newly crystallized form subsequently melted at 189°C, consistent with transformation to form I. Raman spectroscopy of form IV that was heated to 170°C to allow the transformation confirmed that form I had crystallized. This broad transition was also seen in DSC experiments and integration of the form I peak indicates incomplete transformation. DSC also revealed that enthalpy of melting of form IV is 21.4(18) kJ/mol, which establishes a monotropic relationship between forms I and IV and also between forms II and IV based on the application of the heat-of-fusion rule.²⁷

CONCLUSION

Polymer-induced heteronucleation methodology has been demonstrated to selectively crystallize polymorphs of the extensively studied pharmaceuticals FBP and SUL. This approach facilitated the growth of single crystals and subsequent structure determination of two polymorphs that were grown directly from polymers, a result that is highly desirable for unambiguous and accurate characterization of polymorphs. A new polymorph of SUL was also discovered through the application of this technique and its scale-up was achieved by conditions identified through high-throughput screening experiments. Furthermore, the selective growth of a new hydrate of FBP, which could not be produced in the absence of added polymers even with added water in solution, was achieved. These findings indicate that

the polymer-induced heteronucleation approach is of great utility not only for pure compounds but also for multicomponent crystalline solids as well.

ACKNOWLEDGMENTS

This work was supported by the National Institutes of Health (GM072737) and the Alfred P. Sloan Foundation. The authors thank Dr. Jeff W. Kampf for crystal structure determination.

REFERENCES

1. Brittain HG. 1999. Polymorphism in pharmaceutical solids. New York: Marcel Dekker.
2. Bernstein J. 2002. Polymorphism in molecular crystals. New York: Oxford.
3. Byrn S, Pfeiffer R, Ganey M, Hoiberg C, Poochikian G. 1995. Pharmaceutical solids: A strategic approach to regulatory considerations. *Pharm Res* 12:945–954.
4. Price CP, Grzesiak AL, Lang M, Matzger AJ. 2002. Polymorphism of nabumetone. *Cryst Growth Des* 2:501–503.
5. Price CP, Grzesiak AL, Kampf JW, Matzger AJ. 2003. Maize 1: A trimorphic azo pigment. *Cryst Growth Des* 3:1021–1025.
6. Rodríguez-Spong B, Price CP, Jayasankar A, Matzger AJ, Rodríguez-Hornedo N. 2004. General principles of pharmaceutical solid polymorphism: A supramolecular perspective. *Adv Drug Delivery Rev* 56:241–274.
7. Weissbuch I, Popovitz-Biro R, Lahav M, Leiserowitz L. 1995. Understanding and control of nucleation, growth, habit, dissolution and structure of 2-dimensional and 3-dimensional crystals using tailor-made auxiliaries. *Acta Crystallogr Sect B* 51:115–148.
8. Bonafede SJ, Ward MD. 1995. Selective nucleation and growth of an organic polymorph by ledge-directed epitaxy on a molecular-crystal substrate. *J Am Chem Soc* 117:7853–7861.
9. Mitchell CA, Yu L, Ward MD. 2001. Selective nucleation and discovery of organic polymorphs through epitaxy with single crystal substrates. *J Am Chem Soc* 123:10830–10839.
10. Zaccaro J, Matic J, Myerson AS, Garetz BA. 2001. Nonphotochemical, laser-induced nucleation of supersaturated aqueous glycine produces unexpected γ -polymorph. *Cryst Growth Des* 1:5–8.
11. Chyall LJ, Tower JM, Coates DA, Houston TL, Childs SL. 2002. Polymorph generation in capillary spaces: The preparation and structural analysis of a metastable polymorph of nabumetone. *Cryst Growth Des* 2:505–510.

12. Hilden JL, Reyes CE, Kelm MJ, Tan JS, Stowell JG, Morris KR. 2003. Capillary precipitation of a highly polymorphic organic compound. *Cryst Growth Des* 3:921–926.
13. Ha JM, Wolf JH, Hillmyer MA, Ward MD. 2004. Polymorph selectivity under nanoscopic confinement. *J Am Chem Soc* 126:3382–3383.
14. Lee AY, Lee IS, Dettet SS, Boerner J, Myerson AS. 2005. Crystallization on confined engineered surfaces: A method to control crystal size and generate different polymorphs. *J Am Chem Soc* 127:14982–14983.
15. Hiremath R, Basile JA, Varney SW, Swift JA. 2005. Controlling molecular crystal polymorphism with self-assembled monolayer templates. *J Am Chem Soc* 127:18321–18327.
16. Lang M, Grzesiak AL, Matzger AJ. 2002. The use of polymer heteronuclei for crystalline polymorph selection. *J Am Chem Soc* 124:14834–14835.
17. Price CP, Grzesiak AL, Matzger AJ. 2005. Crystalline polymorph selection and discovery with polymer heteronuclei. *J Am Chem Soc* 127:5512–5517.
18. Grzesiak AL, Uribe FJ, Ockwig NW, Yaghi OM, Matzger AJ. 2006. Polymer-induced heteronucleation for the discovery of new extended solids. *Angew Chem Int Edit* 45:2553–2556.
19. Grzesiak AL, Matzger AJ. 2007. Selection and discovery of polymorphs of platinum complexes facilitated by polymer-induced heteronucleation. *Inorg Chem* 46:453–457.
20. Lacoulonche F, Chauvet A, Masse J. 1997. An investigation of flurbiprofen polymorphism by thermoanalytical and spectroscopic methods and a study of its interactions with poly-(ethylene glycol) 6000 by differential scanning calorimetry and modelling. *Int J Pharm* 153:167–179.
21. Lacoulonche F, Chauvet A, Masse J, Egea MA, Garcia ML. 1998. An investigation of FB interactions with poly(ethylene glycol) 6000, poly(ethylene glycol) 4000, and poly- ϵ -caprolactone by thermoanalytical and spectroscopic methods and modeling. *J Pharm Sci* 87:543–551.
22. Henck JO, Kuhnert-Brandstätter M. 1999. Demonstration of the terms enantiotropy and monotropy in polymorphism research exemplified by flurbiprofen. *J Pharm Sci* 88:103–108.
23. Plakogiannis FM, McCauley JA. 1984. Sulindac. In: Florey K, editor. *Analytical profiles of drug substances*. Vol. 13. London: Academic. pp 573–596.
24. Tros de Ilarduya MC, Martín C, Goñi MM, Martínez-Ohárriz MC. 1997. Polymorphism of sulindac: Isolation and characterization of a new polymorph and three new solvates. *J Pharm Sci* 86:248–251.
25. Flippen JL, Gilardi RD. 1975. (\pm)-2-(2-Fluoro-4-biphenyl)propionic acid (flurbiprofen). *Acta Crystallogr Sect B* 31:926–928.
26. Koo CH, Kim SH, Shin W. 1985. Crystal structure of antiinflammatory sulindac. *Bull Korean Chem Soc* 6:222–224.
27. Burger A, Ramberger R. 1979. On the polymorphism of pharmaceuticals and other organic molecular crystals. I: Theory of thermodynamic rules. *Mikrochim Acta* II:259–271.
28. Selective crystallization of FBP form III was also achieved from cellulose acetate butyrate and ethylene/ethyl acrylate copolymer from ethanol solutions, phenoxy resin from acetonitrile solutions, chlorinated polyisoprene from methanol solutions, poly(tetrafluoroethylene) from ethyl acetate solutions, and vinyl chloride/vinyl acetate 90/10 copolymer from 2-propanol solutions.
29. Carbon-hydrogen bonds for all structures were normalized to 1.083 Å prior to measuring close contacts. For van der Waals radii see: Bondi A 1964. Van der Waals volumes and radii. *J Phys Chem* 68(3):441–451.